PREX-2 Experiment and Results

SPIN 2021, Oct 2021
Donald Jones
Temple University
for the PREX-2 collaboration

PREX-II

JEFFERSON LAB, USA

SCIENCE FINDS A WAY

Jefferson Lab

PREX-2 overview

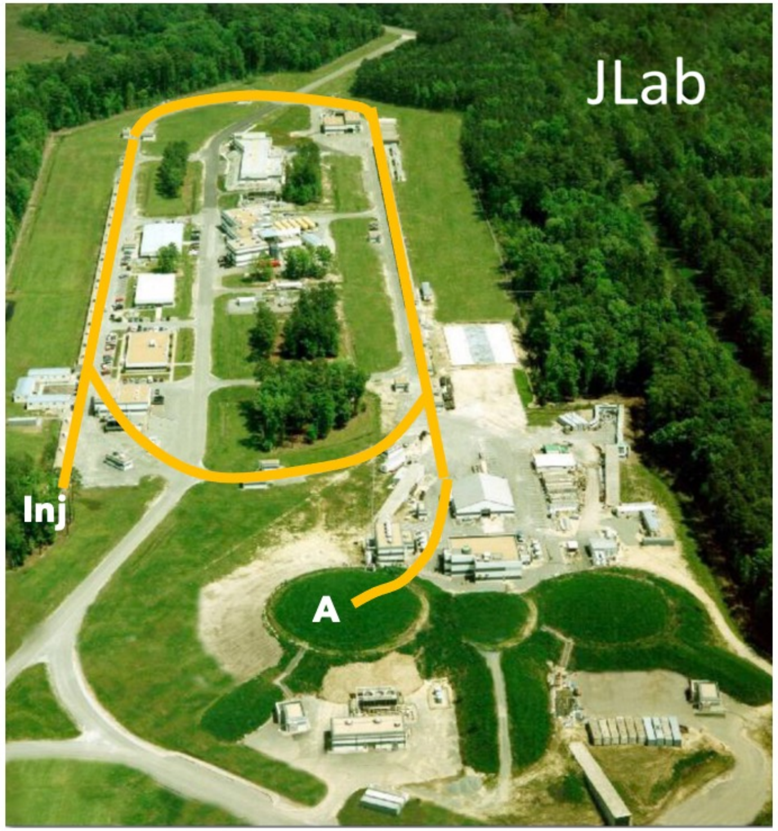

Measured the parity-violating (PV) scattering asymmetry of elastically scattered electrons from the Pb-208 nucleus

Utilized the right/left symmetric high resolution spectrometers (HRS) in Hall A to focus the elastic events

70 µA, 1 GeV electron beam on thin Pb-foil targets

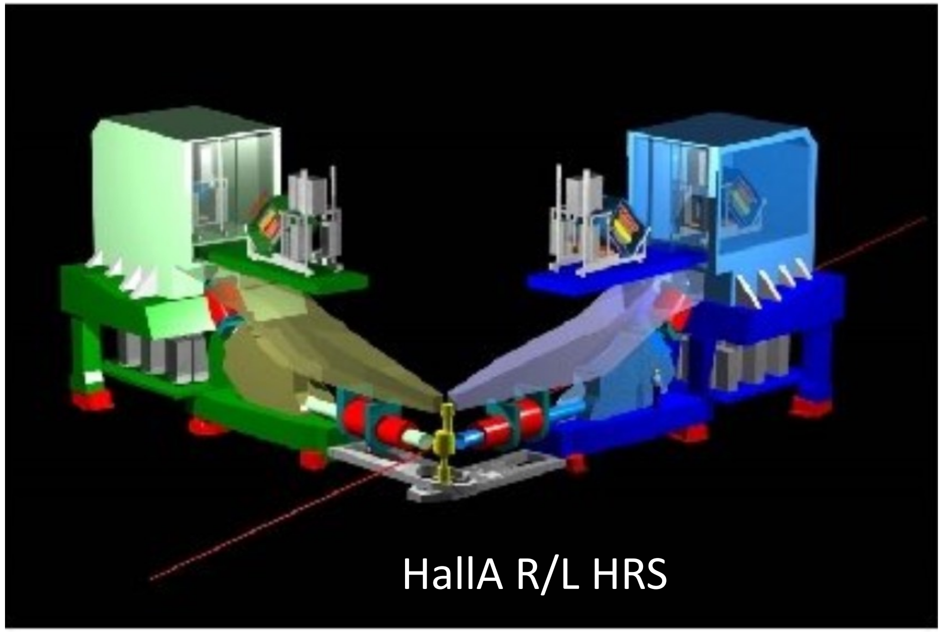

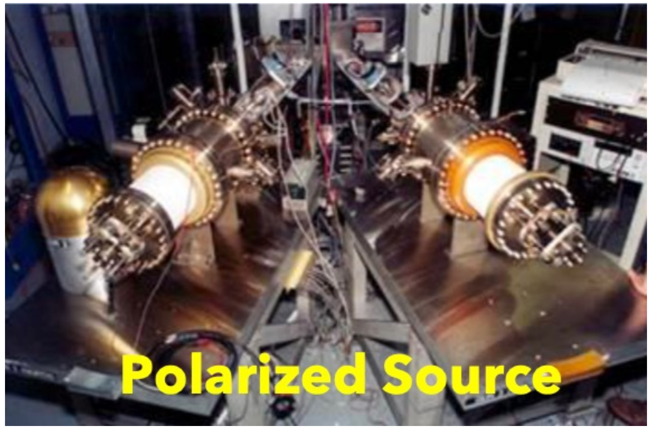

CEBAF currently unique in its capability to run this experiment

Pb-208 neutron distribution via parity violating asymmetry

- Elastic scattering of longitudinally polarized electrons from Pb-208 nucleus
- Parity violating asymmetry sensitive to weak charge i.e. primarily neutron distribution

	Electric	Weak
Proton	1	0.07
Neutron	0	1

- Asymmetry arises from interference term between EM and weak amplitudes

$$A_{PV} \sim \frac{2M_\gamma M_Z}{M_\gamma^2} \sim Q^2 \times 10^{-4}$$

- Flipped electron beam helicity at 120 Hz or 240 Hz and formed asymmetries at 30 Hz.

  120 Hz: $+--+$ *or complement*

  240 Hz: $-++-+--+$ *or complement*

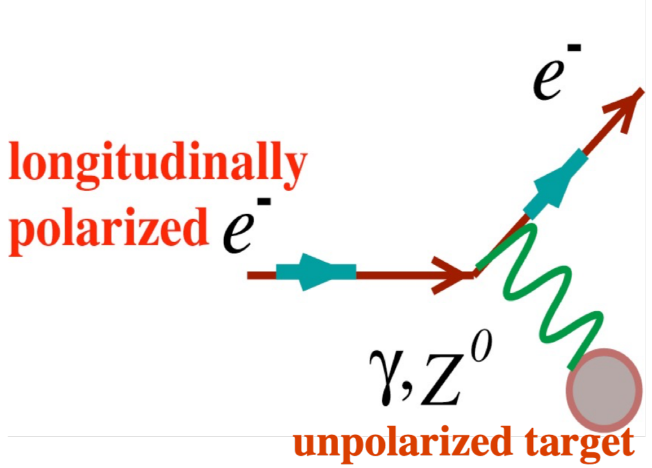

$$A_{PV} = \frac{\sigma_R - \sigma_L}{\sigma_R + \sigma_L}$$

$$\sigma \propto |M_\gamma + M_{weak}|^2$$

$$\sim |M_\gamma|^2 + 2M_\gamma (M_{weak})^* + \ldots$$

$$A_{PV} \approx \frac{G_F Q^2}{4\pi\alpha\sqrt{2}} \frac{Q_W F_W(Q^2)}{Z F_{ch}(Q^2)}$$ (Born Approximation)

Weak Charge Distribution of Heavy Nuclei

Thiel et al J.Phys.G 46 (2019) 9, 093003

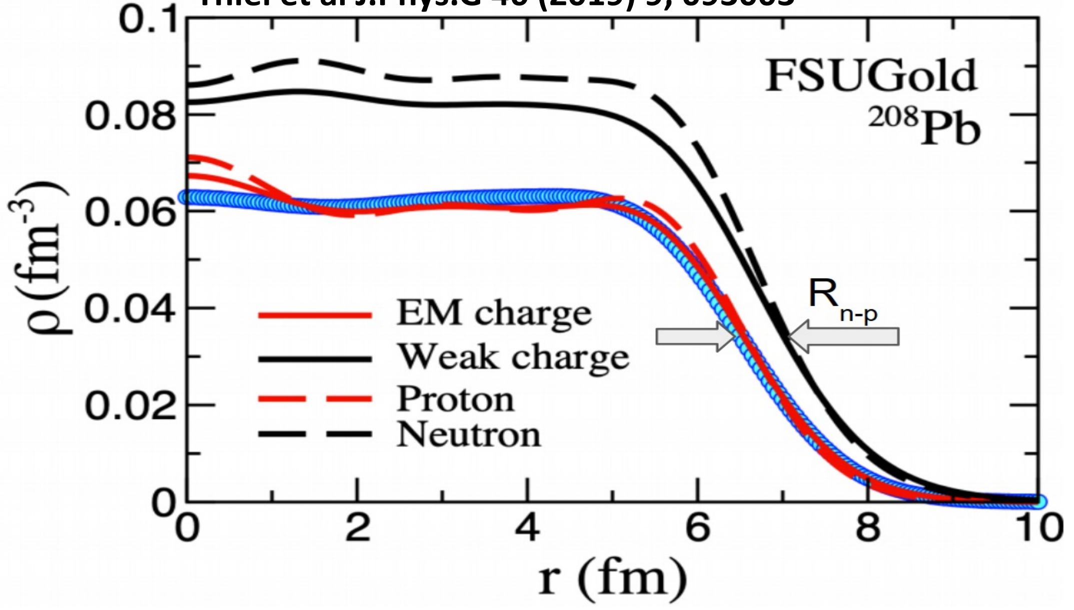

Nuclear theory predicts a neutron "skin" on heavy nuclei

- Neutron skin thickness is highly sensitive to the pressure in neutron-rich matter: constrains EOS
- The greater the pressure (stiffer EOS), the thicker the skin as neutrons are pushed out against surface tension.
- Knowledge of R_n is highly model dependent, and is not well constrained by robust measurements.

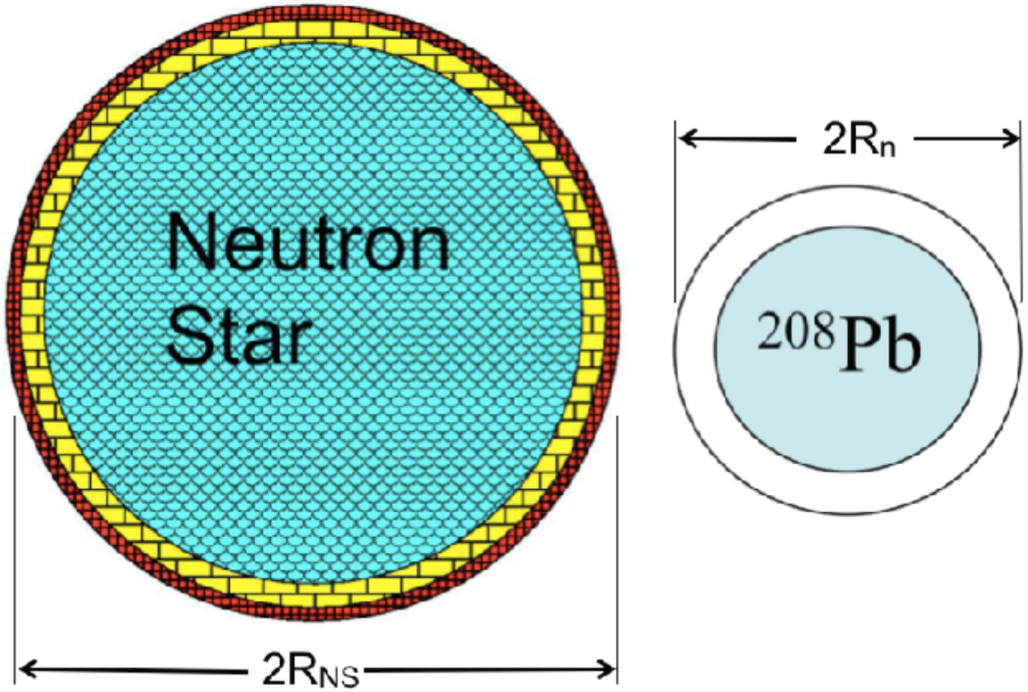

Neutron star is 18 orders of magnitude larger than Pb nucleus but has same neutrons, strong interactions, and equation of state.

Overlap of astro and nuclear physics interests

Neutron EOS parameter *L* connects stars to nuclei

In neutron matter, symmetry energy S (penalty for breaking N=Z) is related to pressure

Pressure:

$$P = \rho^2 \frac{d}{d\rho}\frac{E}{A} \simeq \rho^2 \frac{dS}{d\rho} \simeq \frac{L}{3\rho_0}\rho^2$$

$$L \propto \frac{\delta S(\rho)}{\delta \rho}\Big|_{\rho_0}$$

- Surface relative to core
- Large L=stiff symmetry energy =thick neutron skin
- Star size sensitive to L

PhysRevLett.106.252501

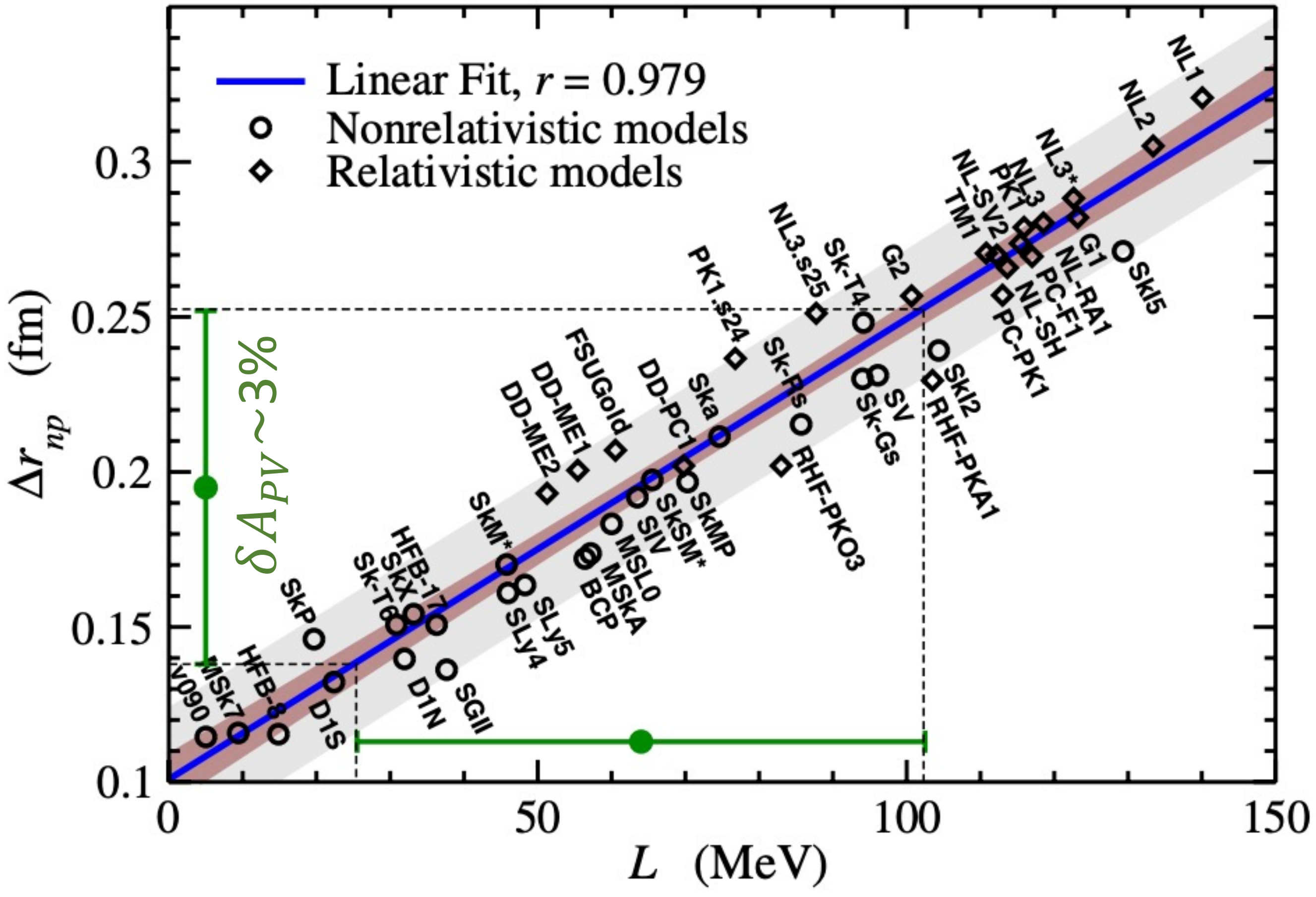

Milestones

- PREX-2 experiment ran from July to early September 2019
- Unblinded results in Sept 2020
- First release talk at DNP Nov 2020
- Published final result in Feb. 2021

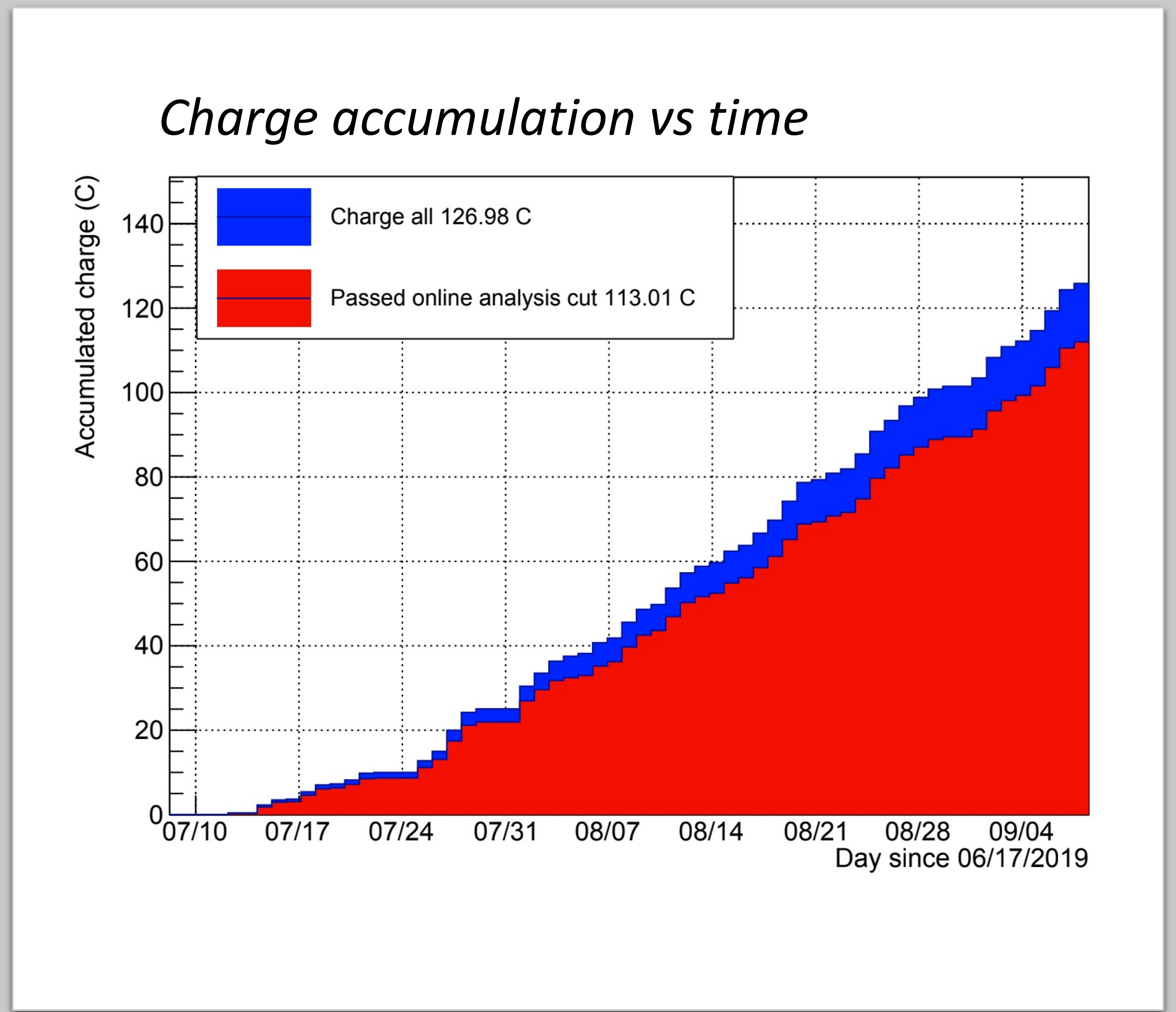

Published Result

- Measured the parity violating elastic scattering asymmetry of electrons from Pb-208 nucleus

- Did better than originally proposed statistical ($\pm$3%) and systematic ($\pm$2%) uncertainty goals*

$$A_{\mathrm{PV}} = 550 \pm 16(\mathrm{stat}) \pm 8\ (\mathrm{syst})\ \text{ppb}$$

**Lower beam energy constraint caused slightly greater error than proposed on neutron radius despite reaching original uncertainty goals.*

Implied neutron skin thickness

$$R_n - R_p = 0.283 \pm 0.071 \text{ fm}$$

Usually need at least two measurements of F(Q) to determine radius from slope near $Q^2 = 0$.

Linear relationship between APV and neutron skin from nuclear structure models allows inference of neutron skin.

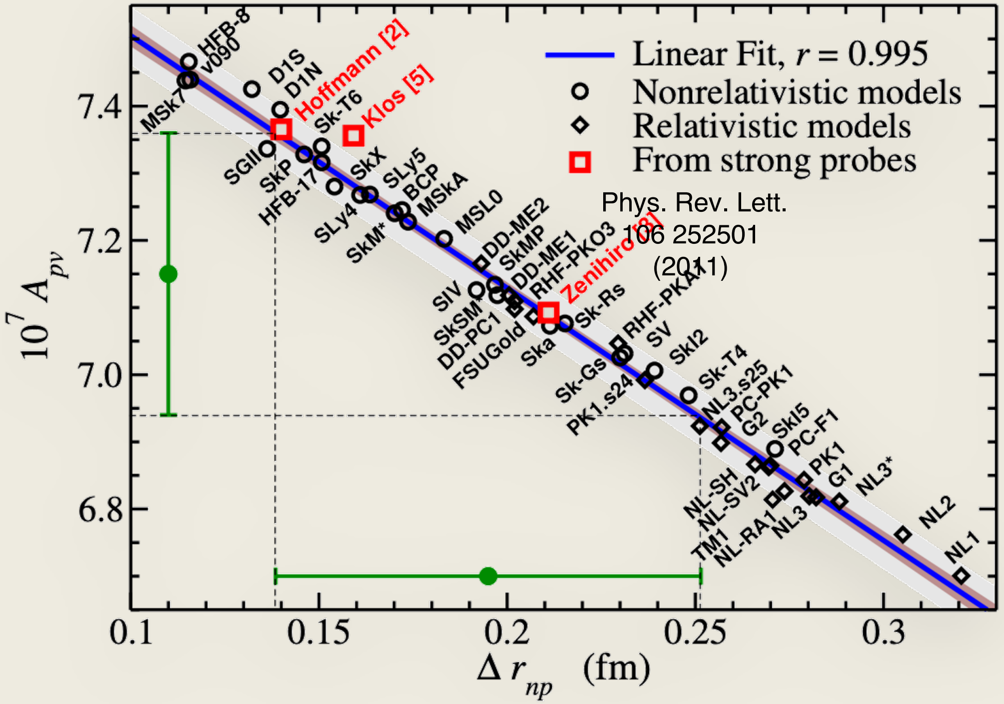

$$A_{PV} \approx \frac{G_F Q^2}{4\pi\alpha\sqrt{2}} \frac{Q_W F_W(Q^2)}{Z F_{ch}(Q^2)} \quad \text{(Born Approximation)}$$

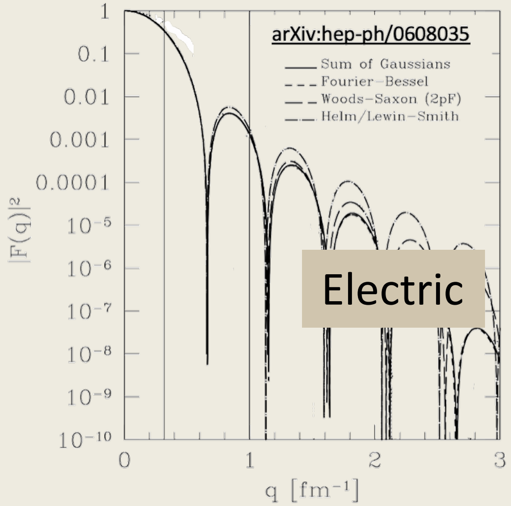

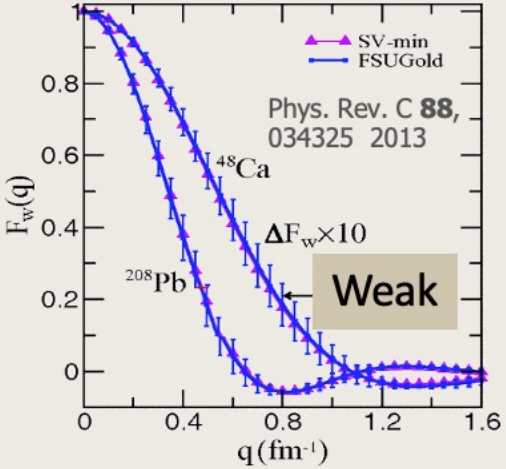

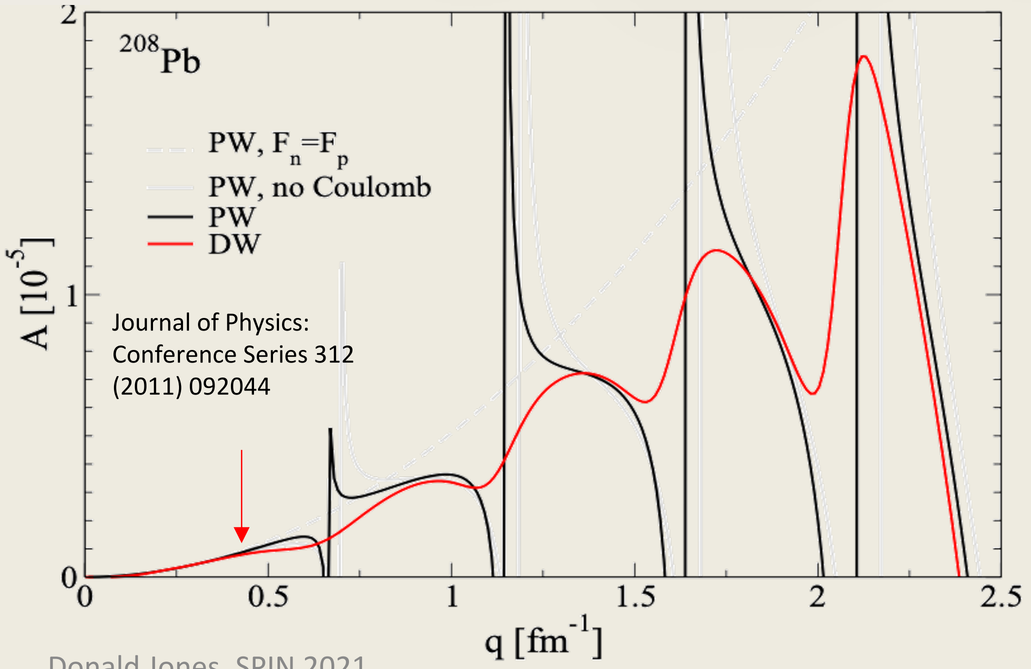

Connecting neutron skin to neutron star radius

Piekarewicz et al arXiv 1907.02561

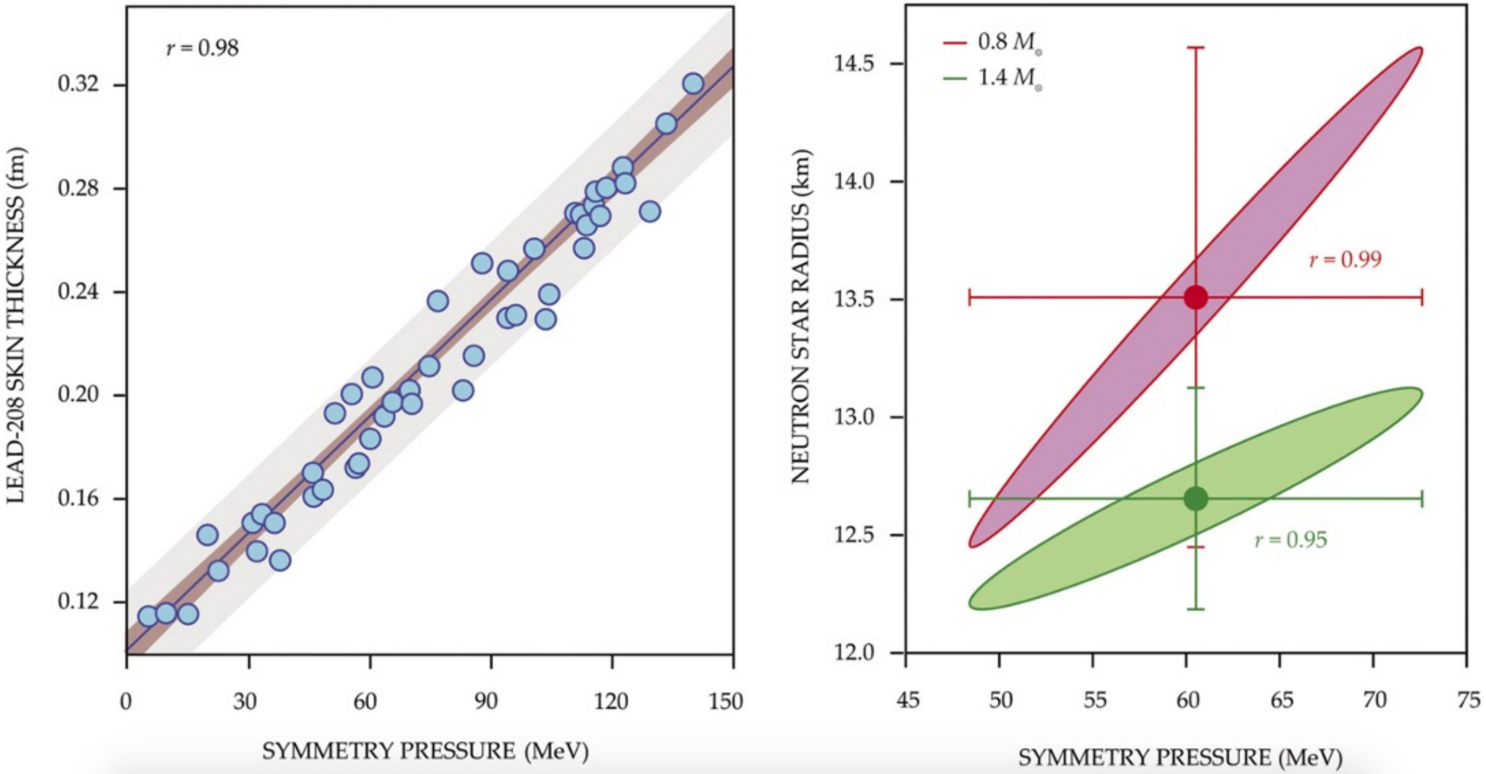

- Although 10^{18} x difference in size, neutron stars and Pb-208 nuclei have same EOS
- Largely unconstrained symmetry energy controls both the neutron skin of Pb-208 and the radius of a neutron star
- Models show strong correlation between R_{Skin}^{208} and R_{Star}
- Neutron skin measured by PREX-2 implies $L = 106 \pm 37$ MeV

Correlation between L and the radii of two neutron stars for different masses.

Neutron star radii

Neutron stars deform in strong gravitational fields parametrized in tidal deformability $\Lambda \sim R^5$

- Soft EOS low maximum mass and small radii
  → deform less = Λ smaller
- Stiff EOS high maximum mass and larger radii
  → deform more = Λ larger

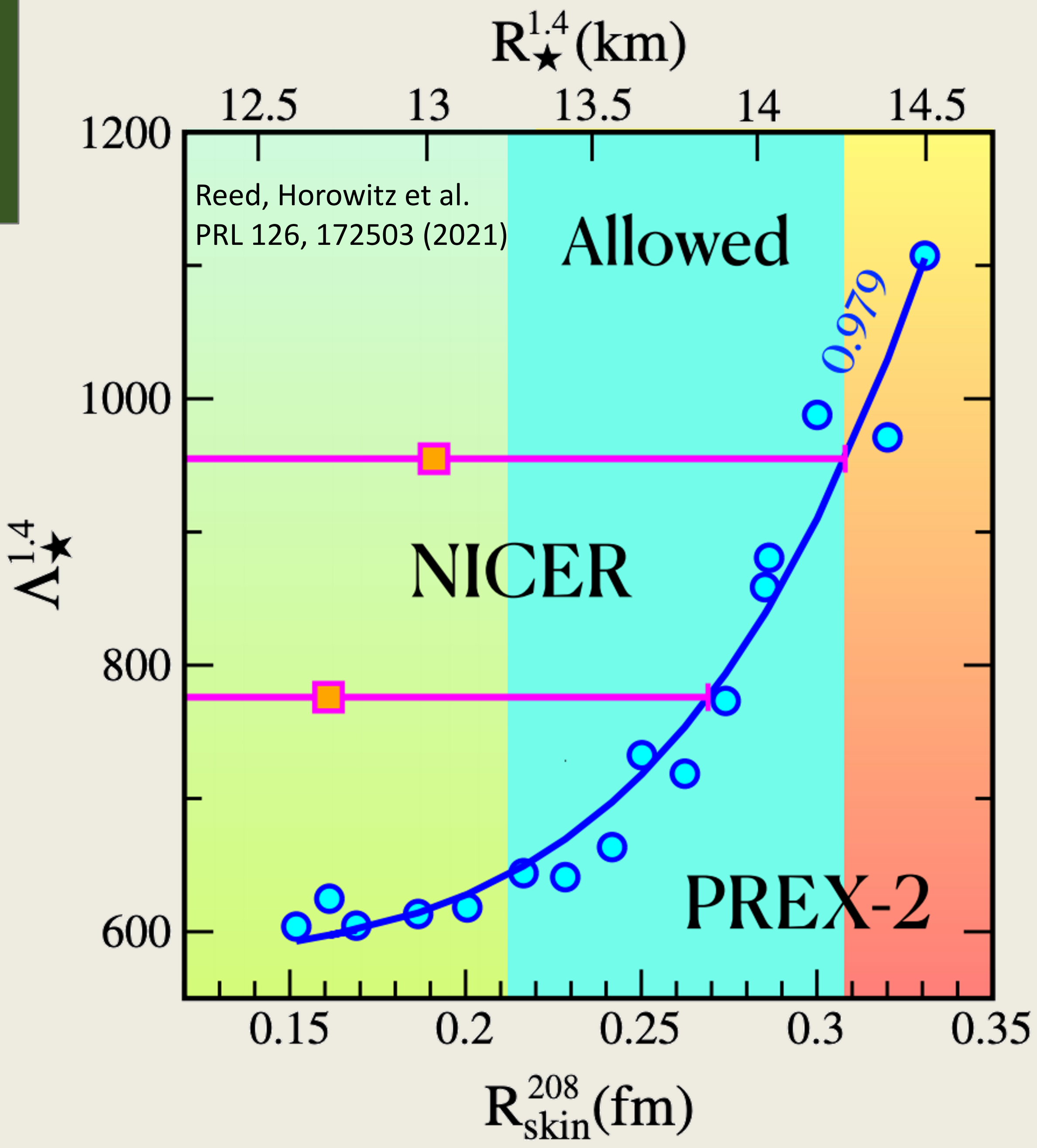

Neutron star radii

Neutron stars deform in strong gravitational fields parametrized in tidal deformability $\Lambda \sim R^5$

- Soft EOS low maximum mass and small radii
  → deform less = Λ smaller
- Stiff EOS high maximum mass and larger radii
  → deform more = Λ larger

- NICER (**N**ASA's neutron star **I**nterior **C**omposition **E**xpore**R**) is an X-ray telescope on the International Space Station
- NICER able to set limit on neutron star radius consistent with PREX

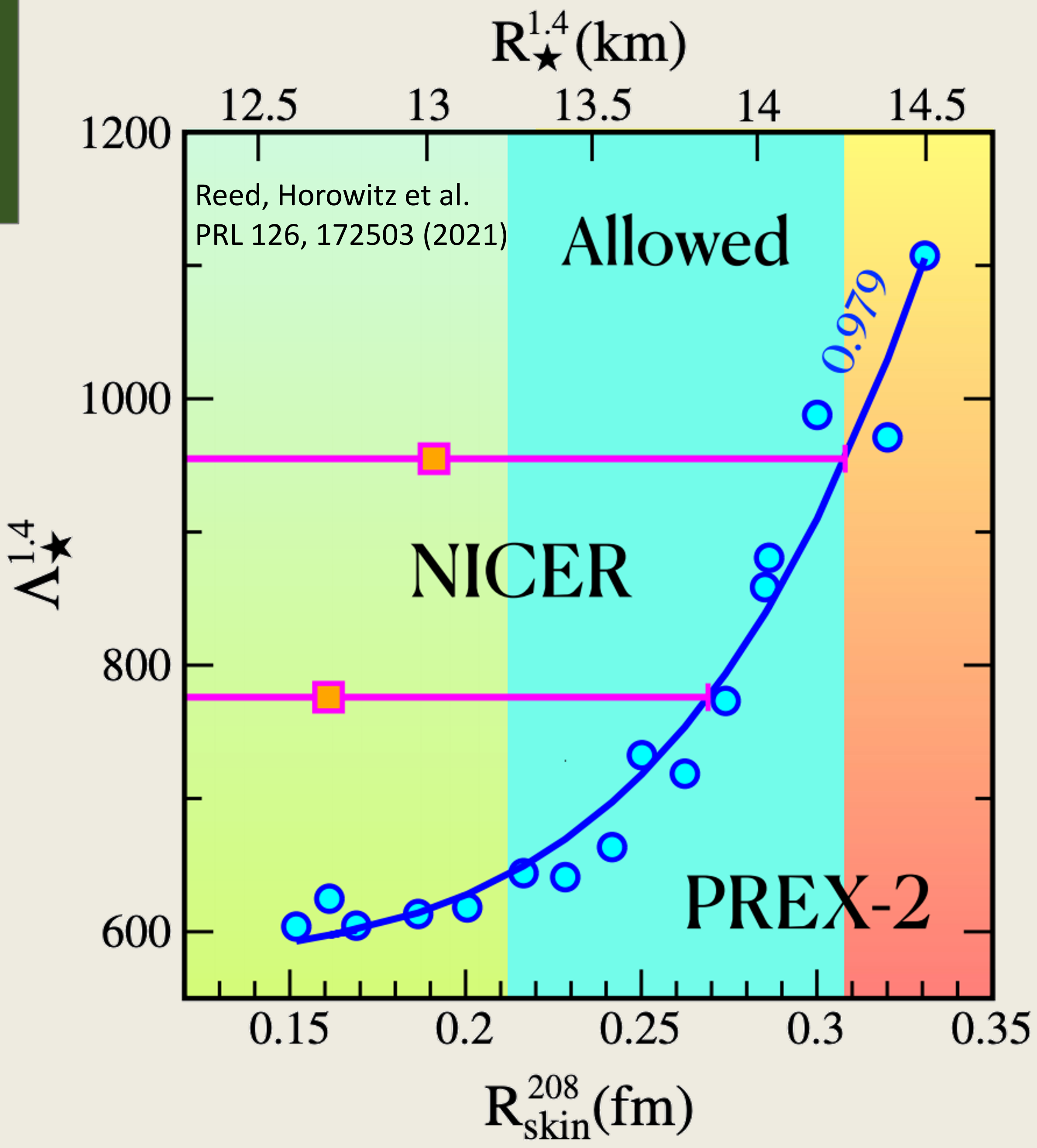

Neutron star radii

Neutron stars deform in strong gravitational fields parametrized in tidal deformability $\Lambda \sim R^5$

- Soft EOS low maximum mass and small radii
  → deform less = Λ smaller
- Stiff EOS high maximum mass and larger radii
  → deform more = Λ larger

- NICER (**N**ASA's neutron star **I**nterior **C**omposition **E**xpore**R**) is an X-ray telescope on the International Space Station
- NICER able to set limit on neutron star radius consistent with PREX

- LIGO determined upper limit on tidal deformability $\Lambda_{1.4} < 580$ for the neutron star merger GW170817 with its gravitational wave measurement (slight tension with PREX)

$$\Lambda_{1.4} = 190^{+390}_{-120}$$ (90% CL)

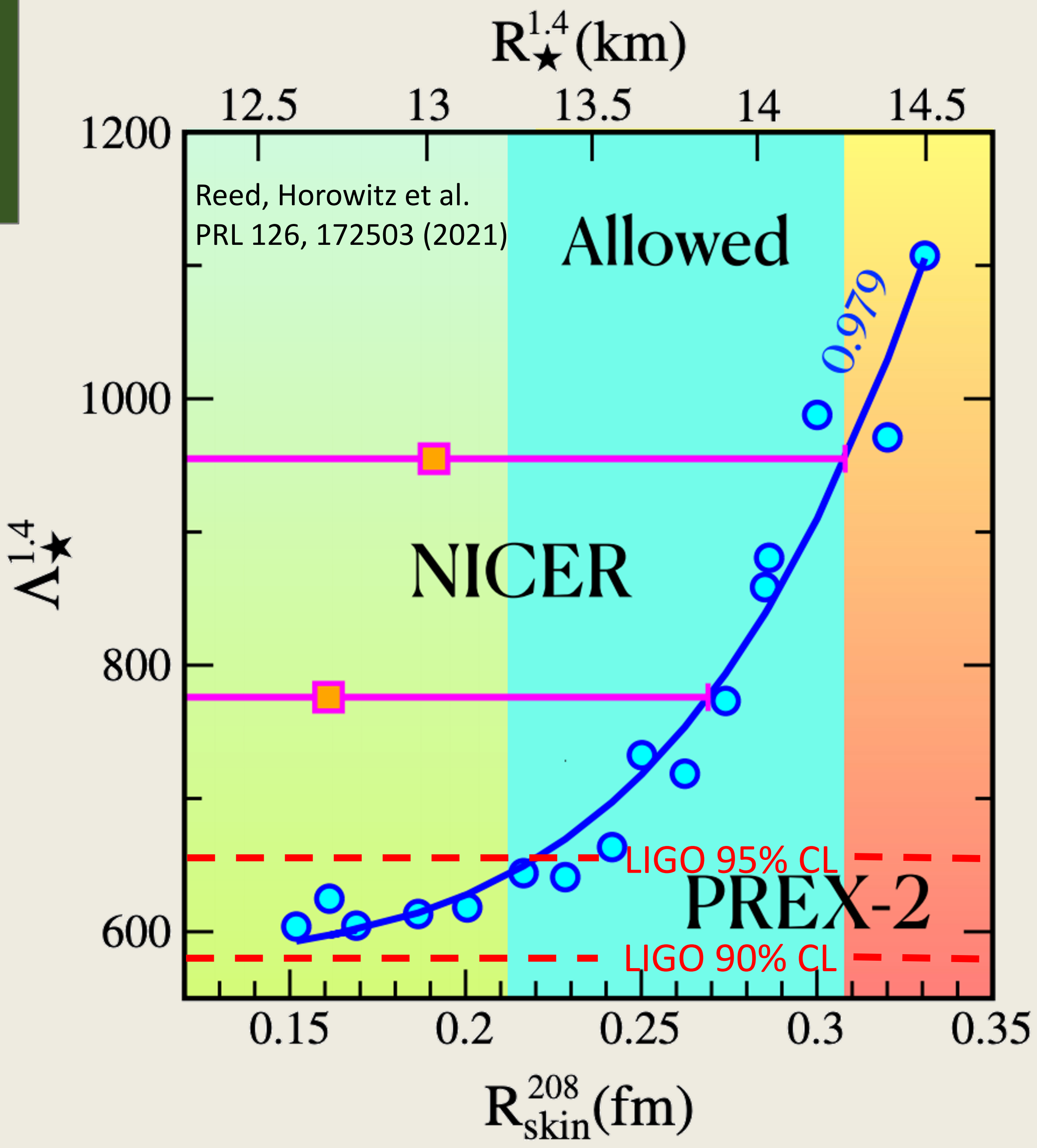

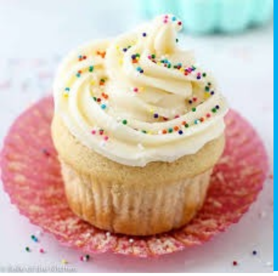

Saturation baryon density

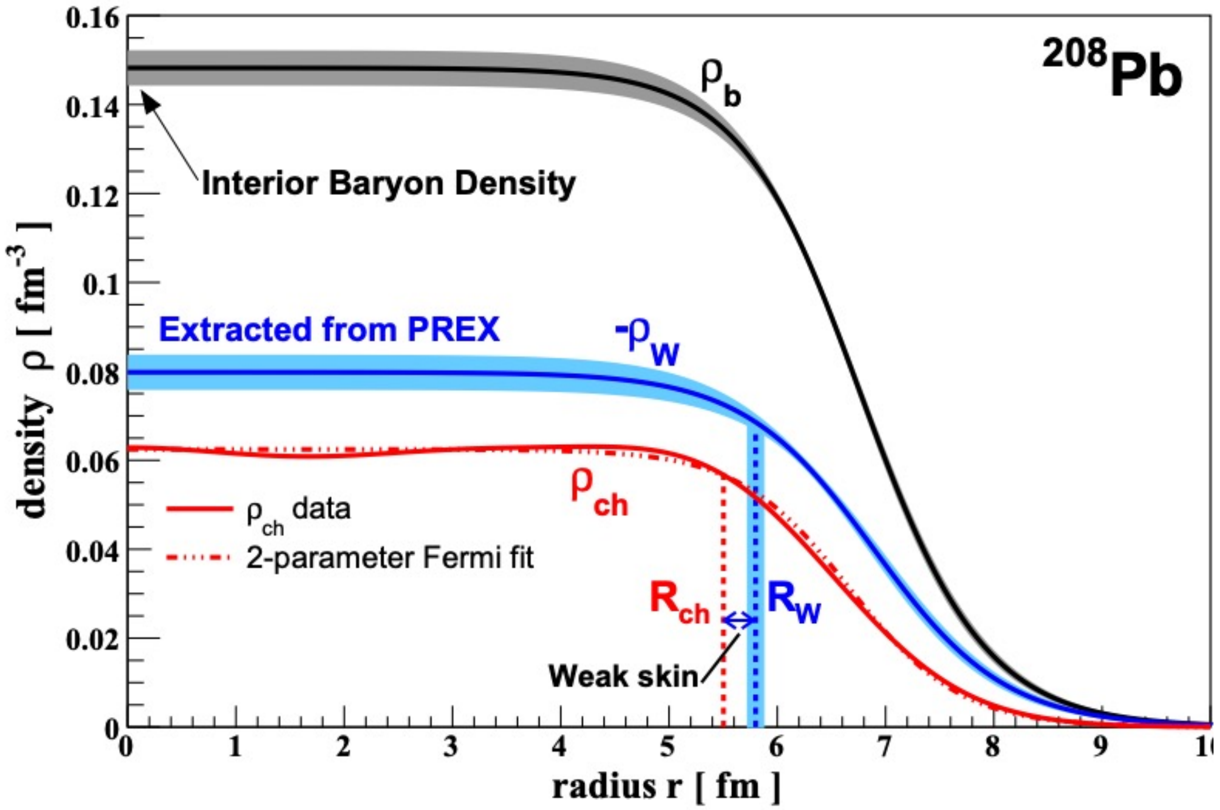

- Nuclear saturation (energy of nuclear matter has a minimum at ρ_0) is fundamental to nuclear structure.
  - Suggested by semi-empirical mass formula.
  - Very hard to calculate even today with Chiral EFT.
- Nuclear saturation suggests interior baryon density of heavy nuclei should be approx. constant and equal to ρ_0.
  - Never cleanly observed.
  - Charge densities known but heaviest stable N=Z nucleus is 40Ca (too small to clearly show saturation).
- Combining weak charge radius from PREX-2 and known electric charge radius able to determine baryon density to better than 3% (theory + exp error)

$$\rho_b^0 = 0.1482 \pm 0.0040 \text{ fm}^{-3}$$

Citations indicate continuing community interest

PREX-1 Published Jan 2012

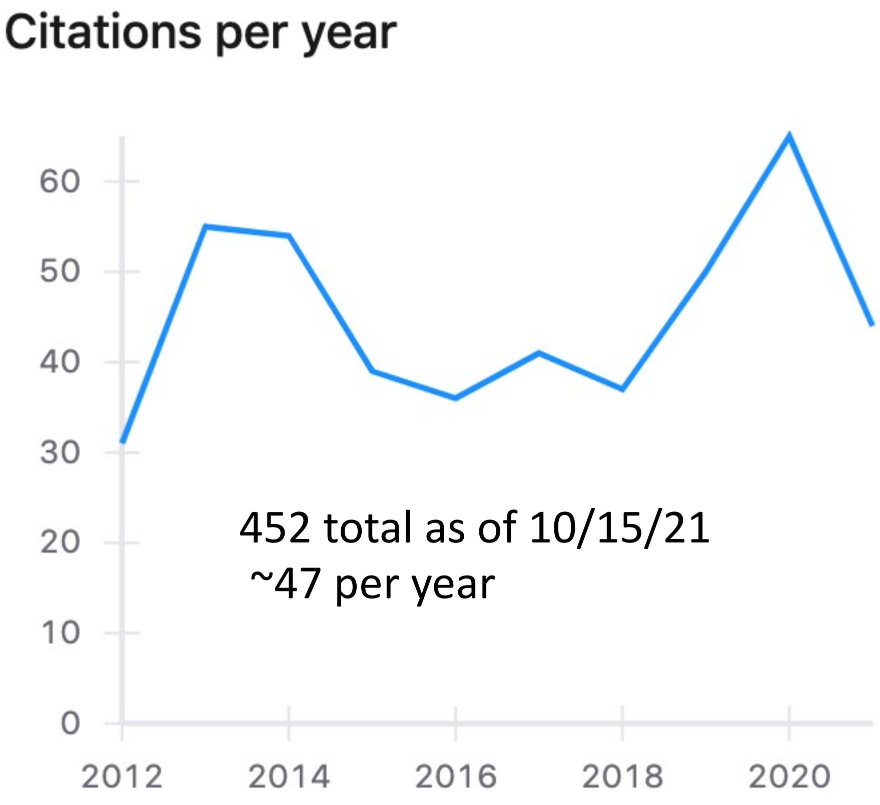

PREX-2 Published Feb 2021

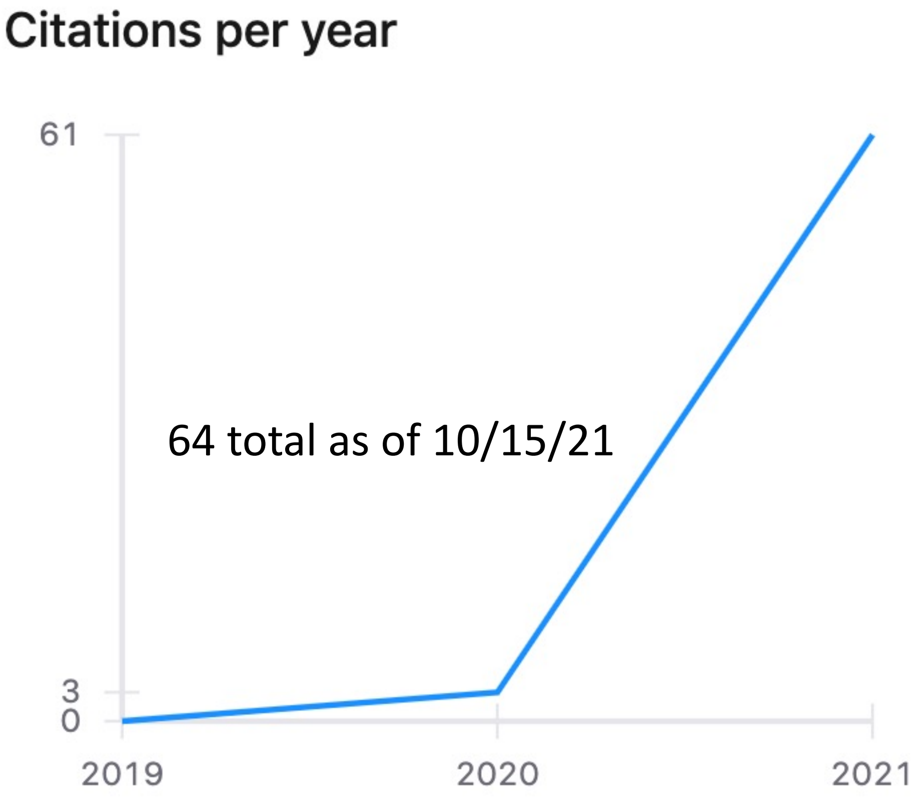

Interest extends well beyond the electron scattering community into nuclear structure and astrophysics

Garnered press attention

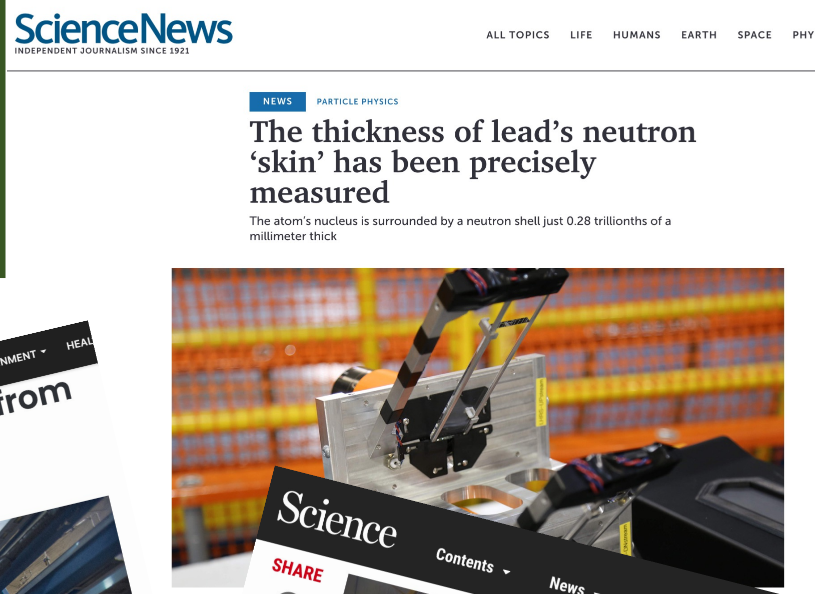

APS Viewpoint "highlighting exceptional research"

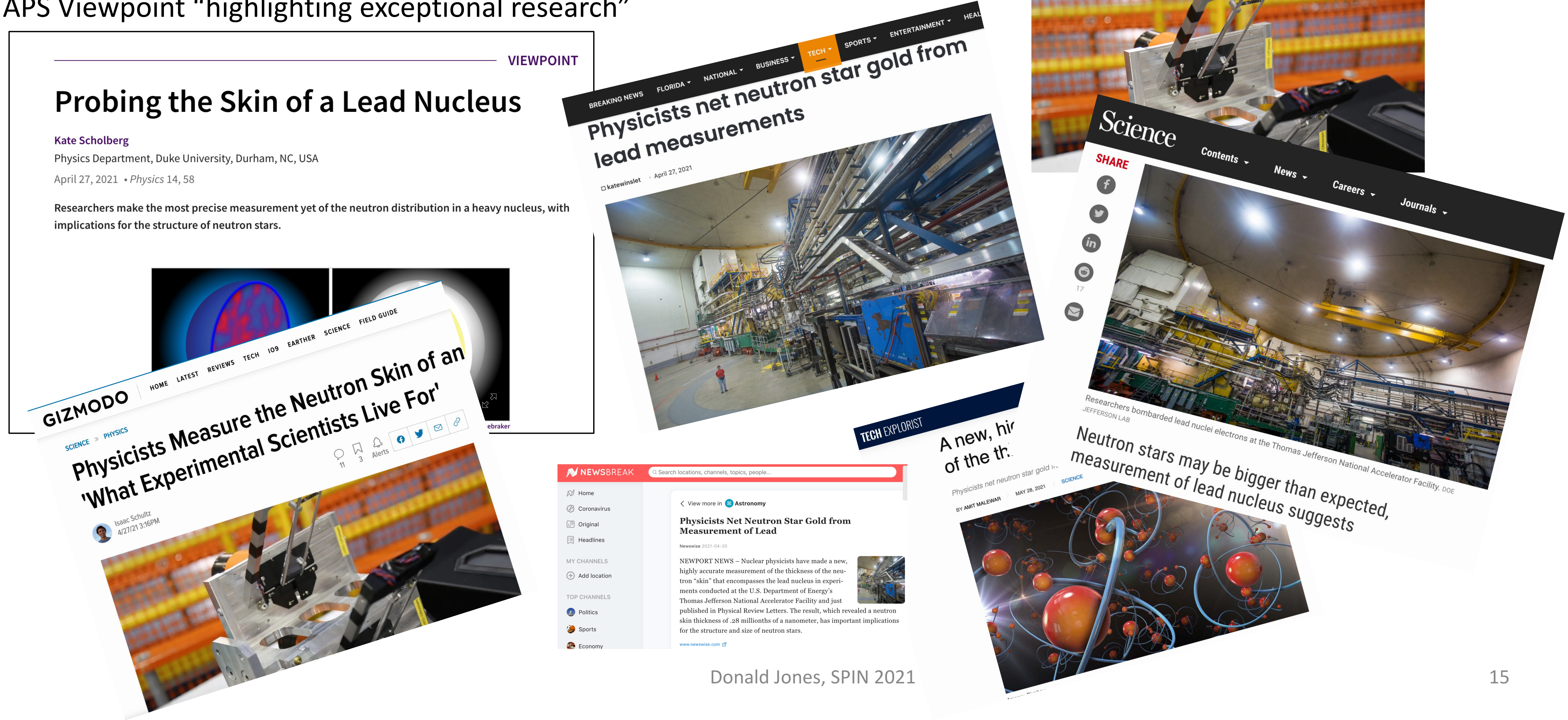

Achieving the physics result

Beam-related false asymmetries

- Changes in beam parameters between helicity states create false asymmetries which could easily be of comparable size to the physics.
  - ->Typical corrections involve beam energy, intensity, XY angle and XY position
- Solution: carefully minimize/cancel false asymmetries and correct residual
- During PREX-2 careful setup and monitoring of the polarized source produced small residual helicity-correlated differences

Δx_i	Mean (nm)
Target x	-1.1 nm
Target y	1.1 nm
Angle x	-0.28 nrad
Angle y	0.14 nrad
Energy BPM	2.3 nm

Correct using measured sensitivities $\frac{\partial A}{\partial x_i}$:

$$A_{PV} = A_{meas} - \sum \frac{\partial A}{\partial x_i} \Delta x_i, \qquad x_i = x, y, x', y', E$$

Total beam corrections:
(60.4 ± 2.5) ppb

$A_{PV} = 550$ ppb

Data quality

- Very close watch on-line data stream - beam conditions, detector response, etc.
- Frequent contact with MCC operators to maintain running conditions
- “prompt" analysis process flagged more subtle problems
- Daily grooming and review in “WAC" process

Corrected asymmetry consistent over experiment after correction

Null asymmetry consistent with 0

Asymmetry after correction for HC beam asymmetries

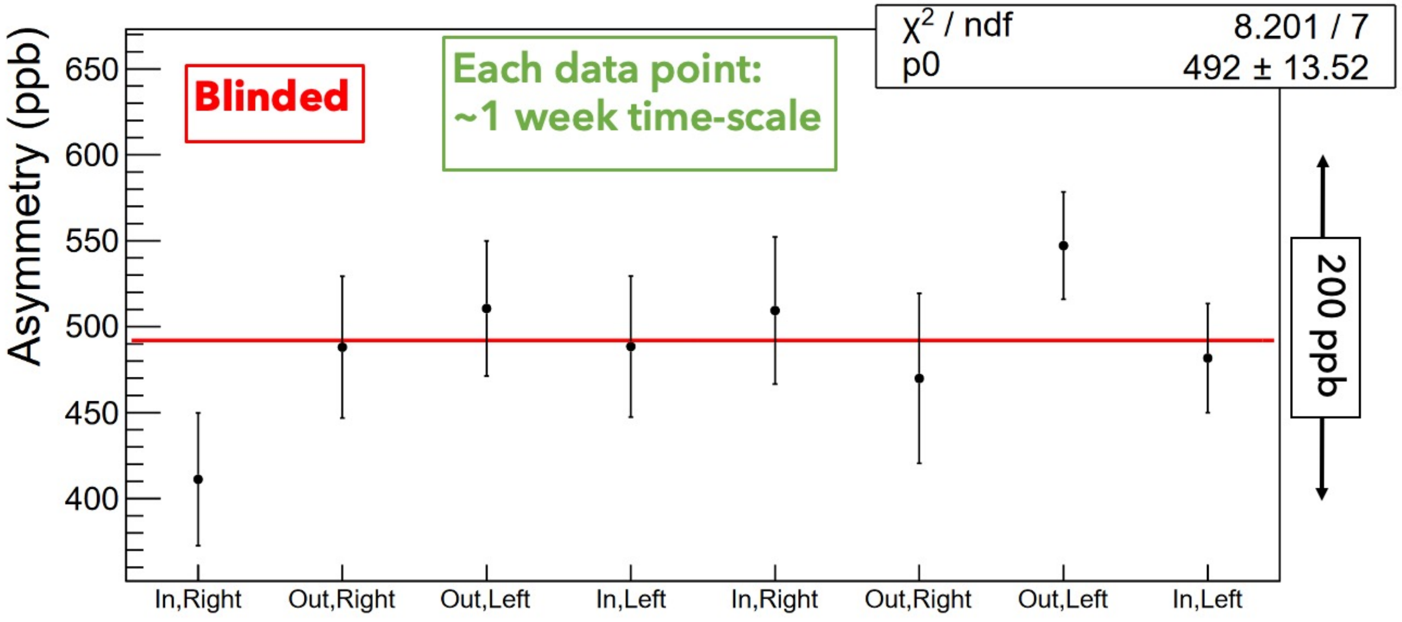

Cancellation of residual false asymmetries with helicity reversals

1. Halfwave plate (In/Out) reverses relative laser helicity
2. Wien reversal (Right/Left) rotates electron launch angle 180 deg

Data quality

- Very close watch on-line data stream - beam conditions, detector response, etc.
- Frequent contact with MCC operators to maintain running conditions
- "prompt" analysis process flagged more subtle problems
- Daily grooming and review in "WAC" process

Corrected asymmetry consistent over experiment after correction

Null asymmetry consistent with 0

Asymmetry after correction for HC beam asymmetries

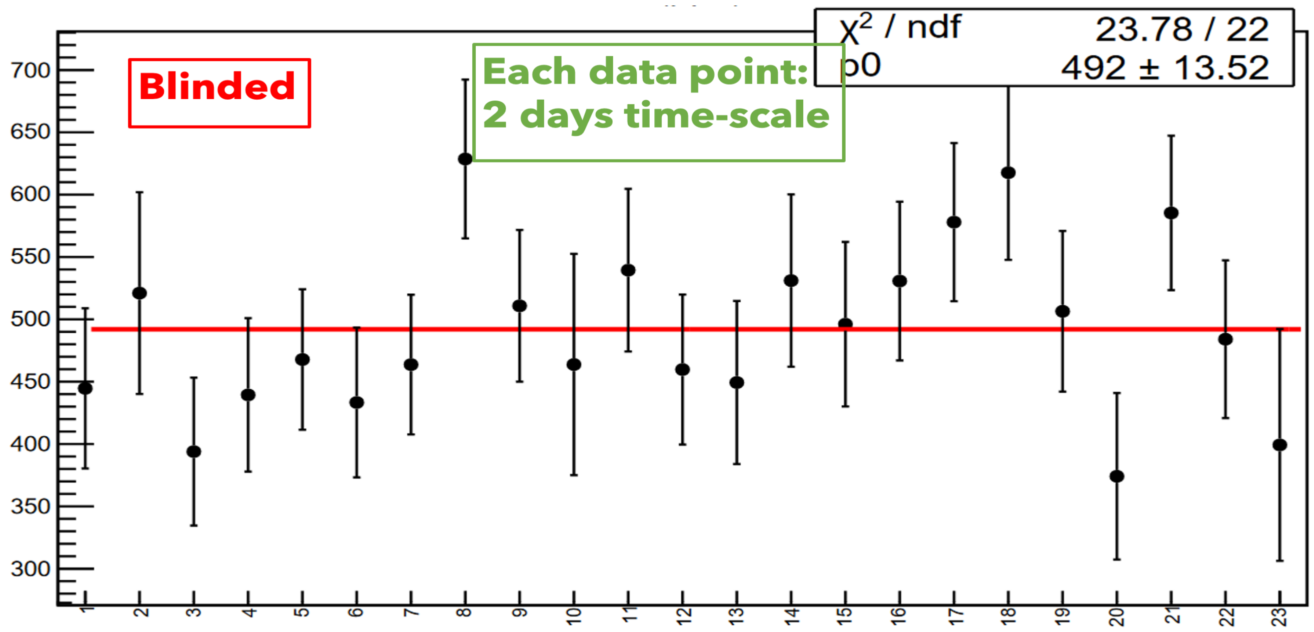

Cancellation of residual false asymmetries with helicity reversals

1. Halfwave plate (In/Out) reverses relative laser helicity
2. Wien reversal (Right/Left) rotates electron launch angle 180 deg

Data quality

- Very close watch on-line data stream - beam conditions, detector response, etc.
- Frequent contact with MCC operators to maintain running conditions
- “prompt" analysis process flagged more subtle problems
- Daily grooming and review in “WAC" process

Corrected asymmetry consistent over experiment after correction

Null asymmetry consistent with 0

Asymmetry after correction for HC beam asymmetries

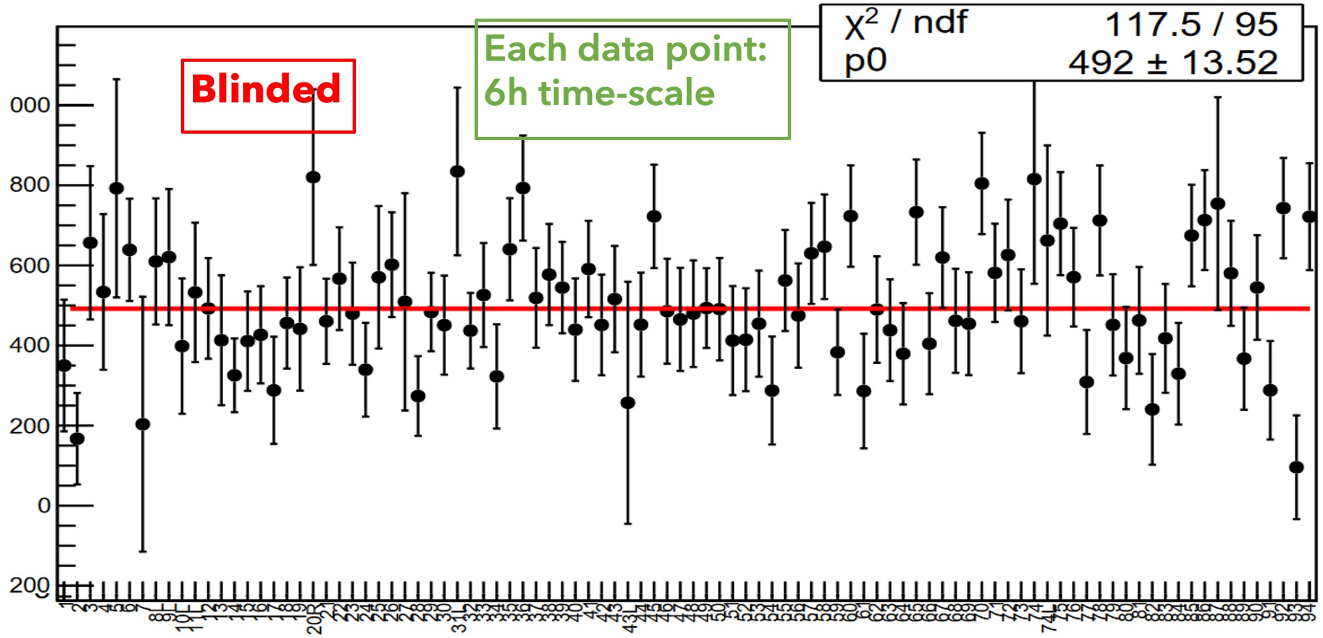

Cancellation of residual false asymmetries with helicity reversals

1. Halfwave plate (In/Out) reverses relative laser helicity
2. Wien reversal (Right/Left) rotates electron launch angle 180 deg

Data quality

- Very close watch on-line data stream - beam conditions, detector response, etc.
- Frequent contact with MCC operators to maintain running conditions
- “prompt" analysis process flagged more subtle problems
- Daily grooming and review in “WAC" process

Corrected asymmetry consistent over experiment after correction

Null asymmetry consistent with 0

Asymmetry after correction for HC beam asymmetries

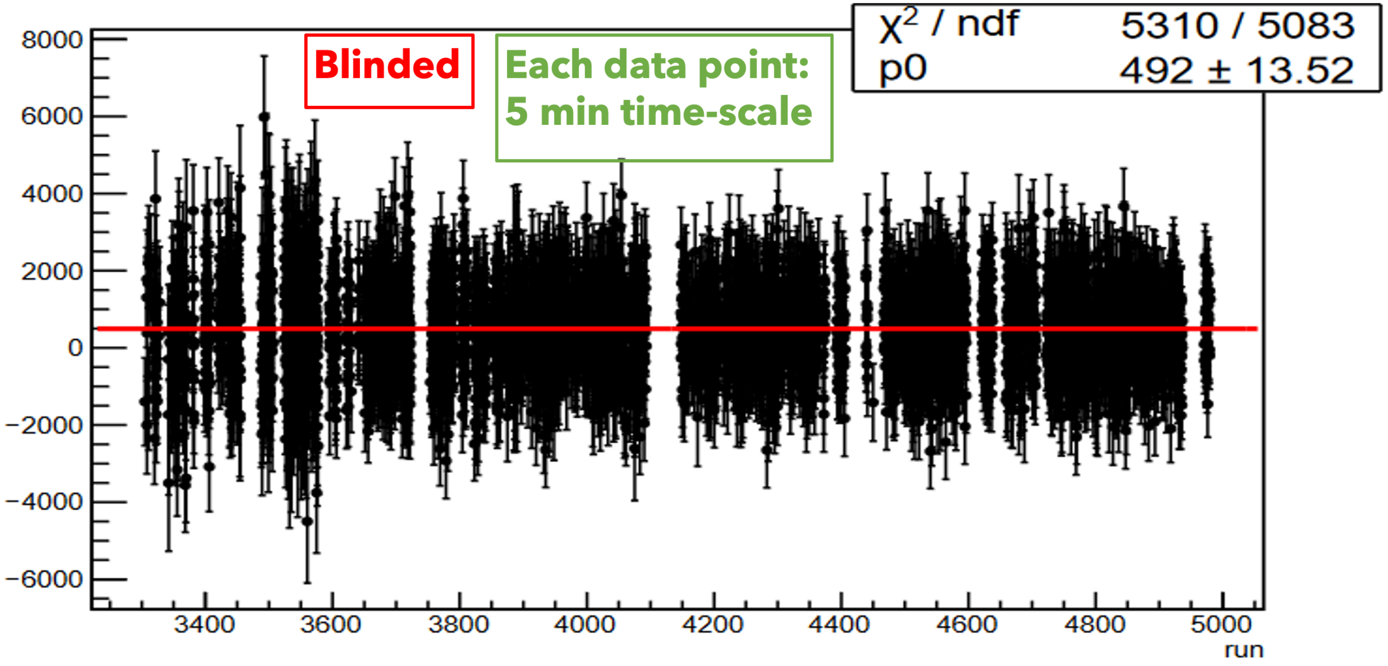

Cancellation of residual false asymmetries with helicity reversals

1. Halfwave plate (In/Out) reverses relative laser helicity
2. Wien reversal (Right/Left) rotates electron launch angle 180 deg

Data quality

- Very close watch on-line data stream - beam conditions, detector response, etc.
- Frequent contact with MCC operators to maintain running conditions
- “prompt" analysis process flagged more subtle problems
- Daily grooming and review in “WAC" process

Asymmetry after correction for HC beam asymmetries

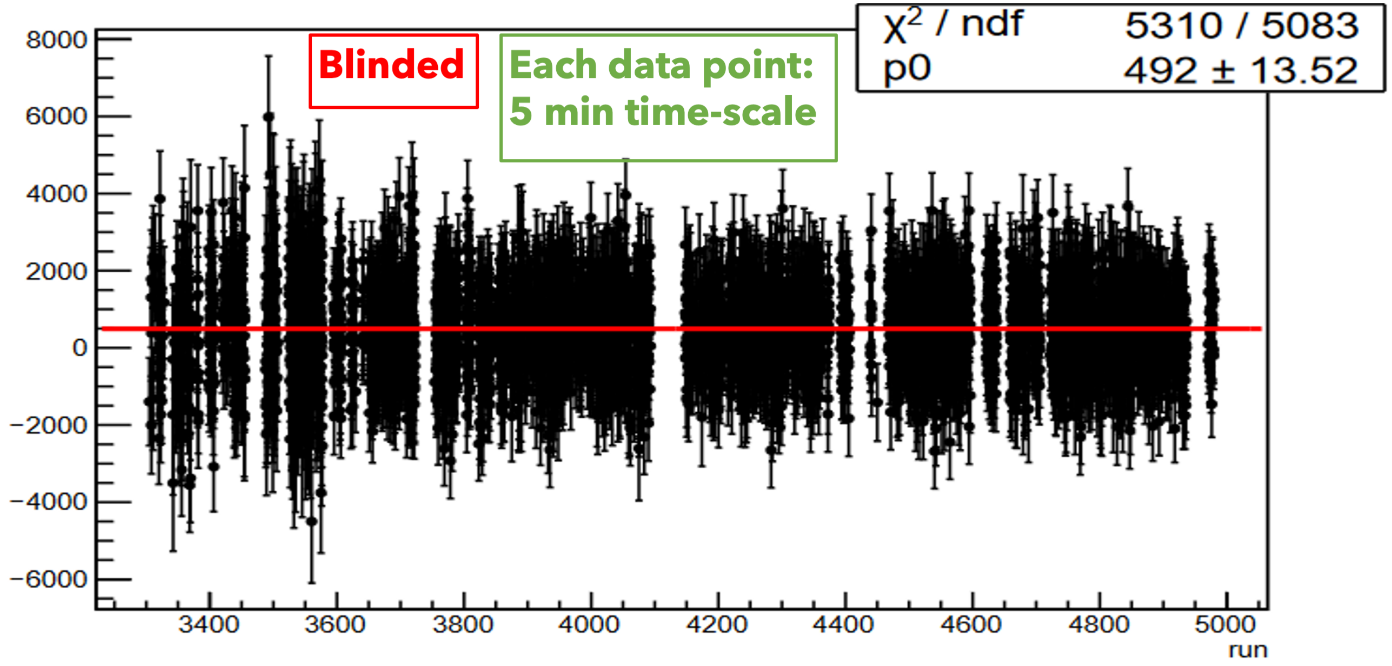

Corrected asymmetry consistent over experiment after correction

Null asymmetry consistent with 0

Cancellation of residual false asymmetries with helicity reversals

1. Halfwave plate (In/Out) reverses relative laser helicity
2. Wien reversal (Right/Left) rotates electron launch angle 180 deg

After correcting for beam asymmetries, need to correct for backgrounds and scale by polarization

$$A_{PV}^{\rm meas} = \frac{1}{P_b}\frac{A_{\rm corr} - P_b\sum_i A_i f_i}{1-\sum_i f_i}$$

Moller polarimetry

- Low-current, invasive measurement
- 3-4T field provides saturated magnetization perpendicular to the foil
- Spectrometer redesigned for 11 GeV

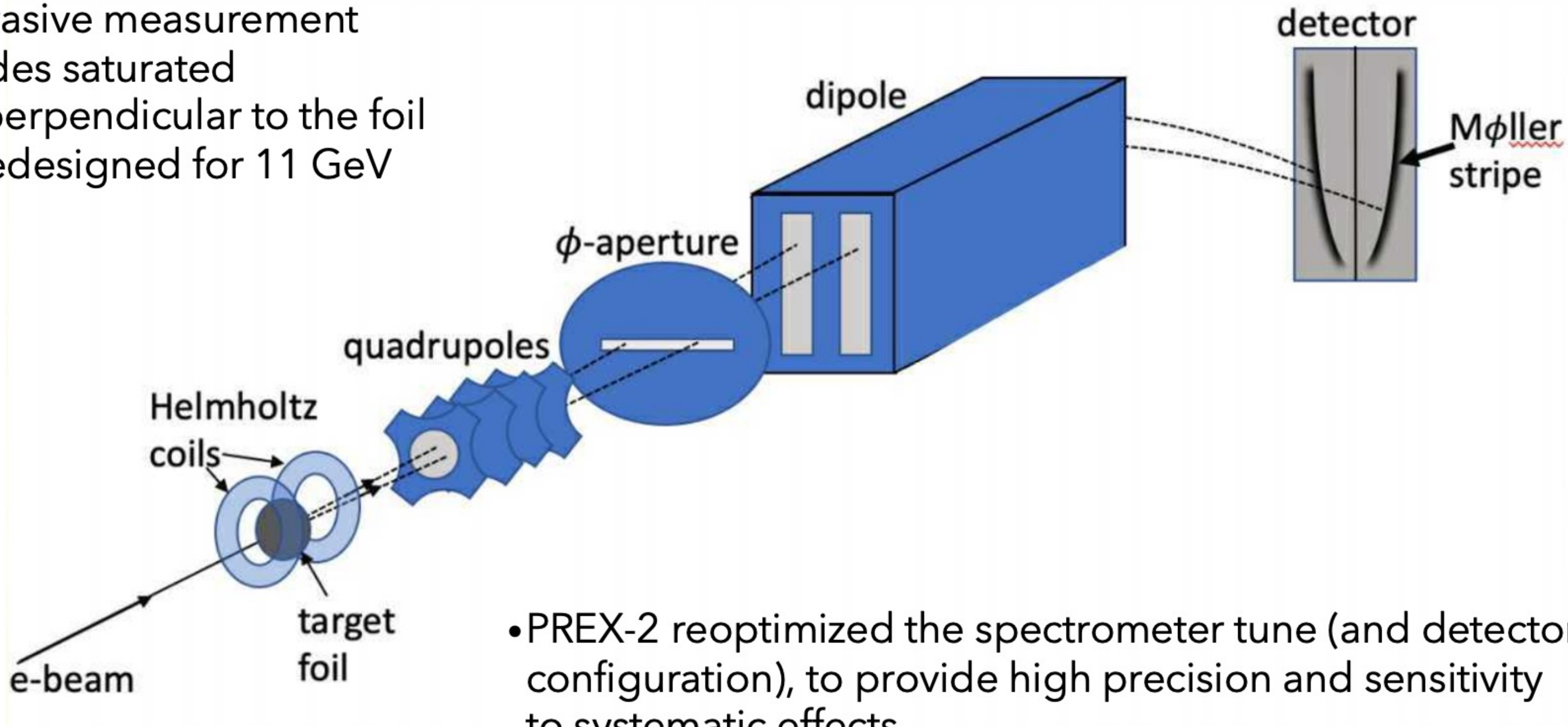

Average polarization:
(89.7 ± 0.8)%

- PREX-2 reoptimized the spectrometer tune (and detector configuration), to provide high precision and sensitivity to systematic effects
- Polarimeter runs were taken approximately every week and established no significant fluctuations in beam polarization over the course of the run
- Cross check with Compton polarimeter was consistent

HRS Spectrometers

- Spectrometer separates elastic peak, directs it onto integrating detector
- Integrate detector in each of the spectrometer pair independently

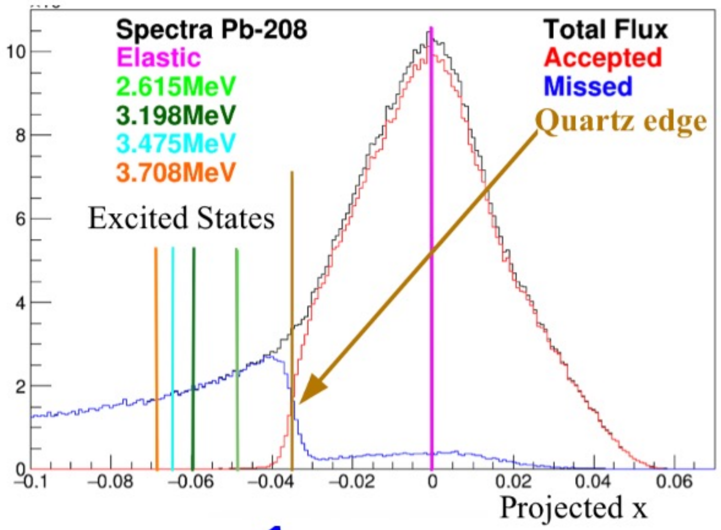

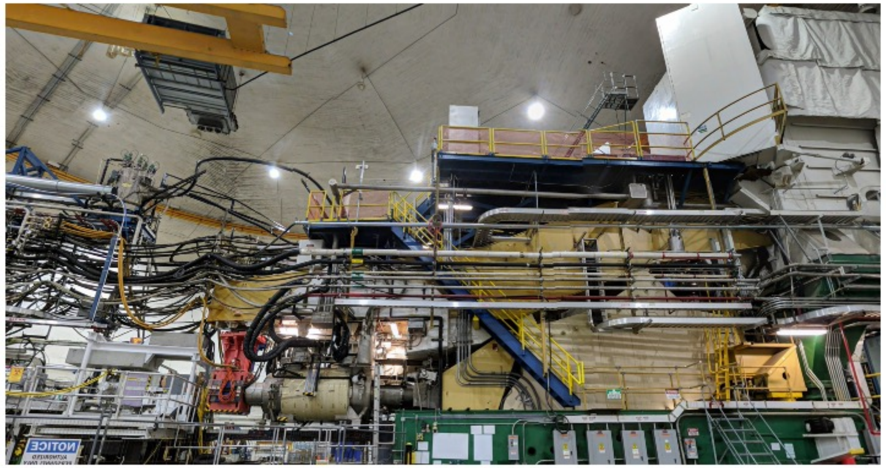

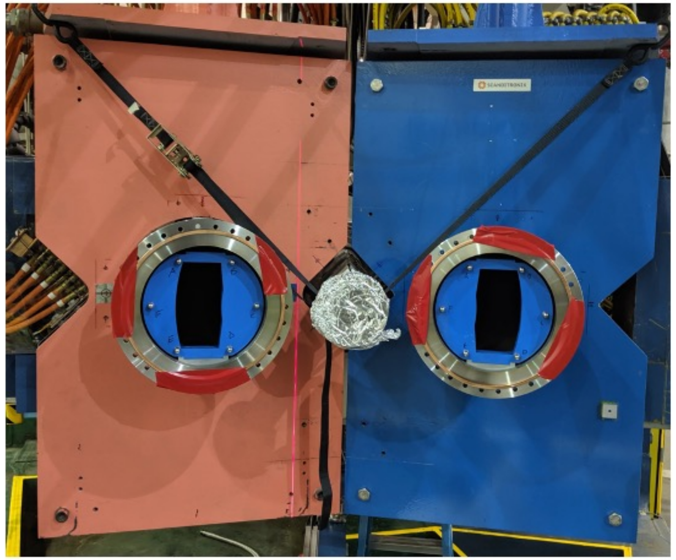

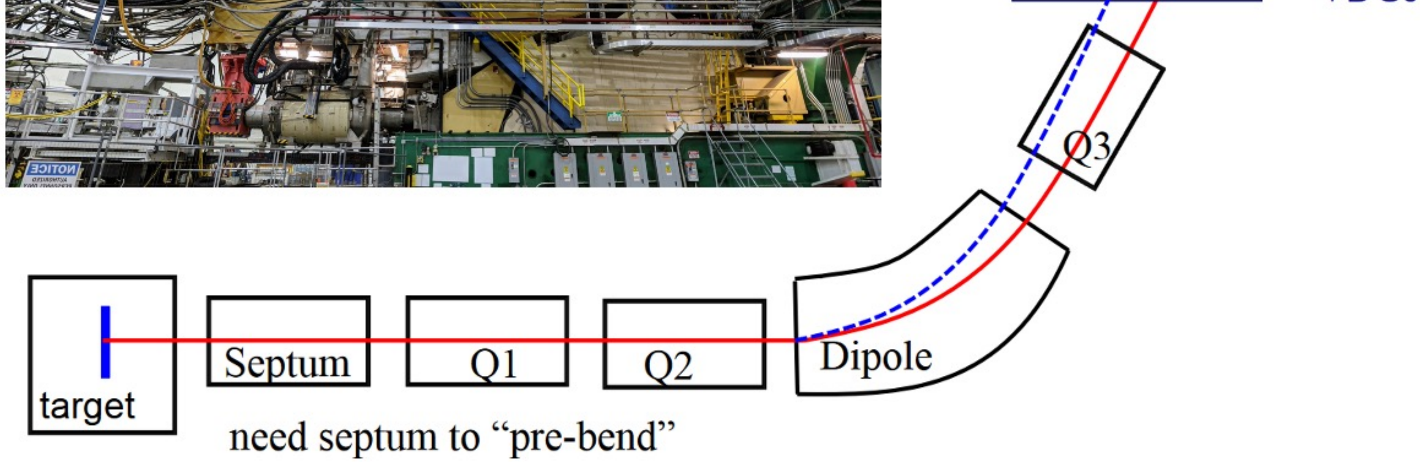

~12.5° Spectrometers

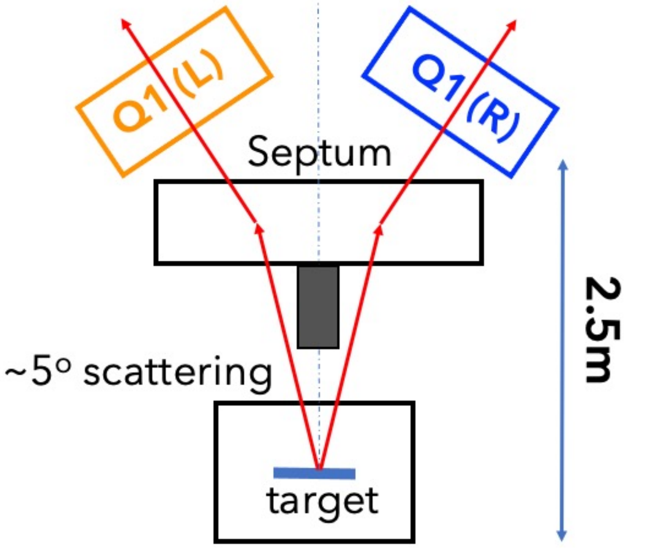

HRS Spectrometers

- Spectrometer separates elastic peak, directs it onto integrating detector
- Integrate detector in each of the spectrometer pair independently

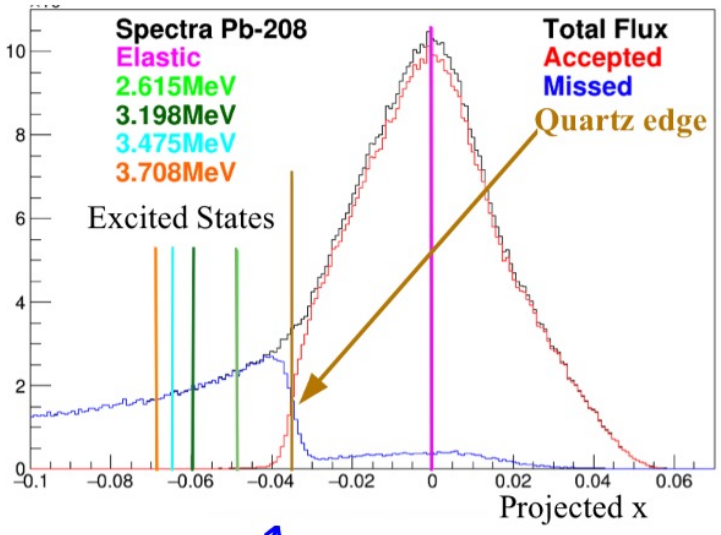

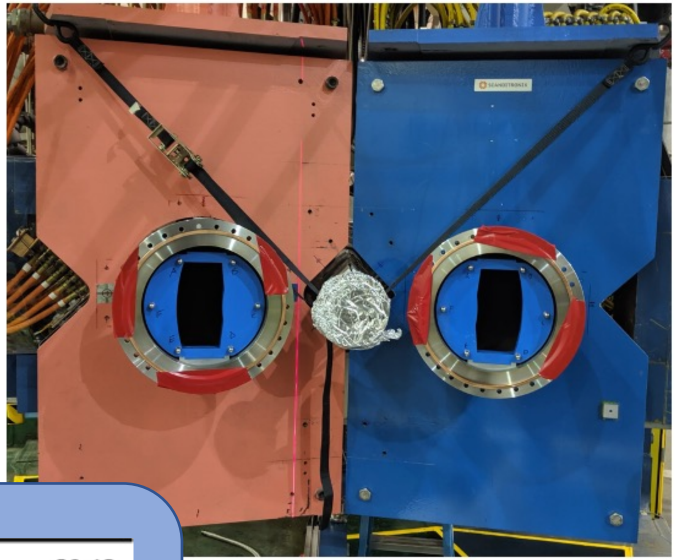

~12.5° Spectrometers

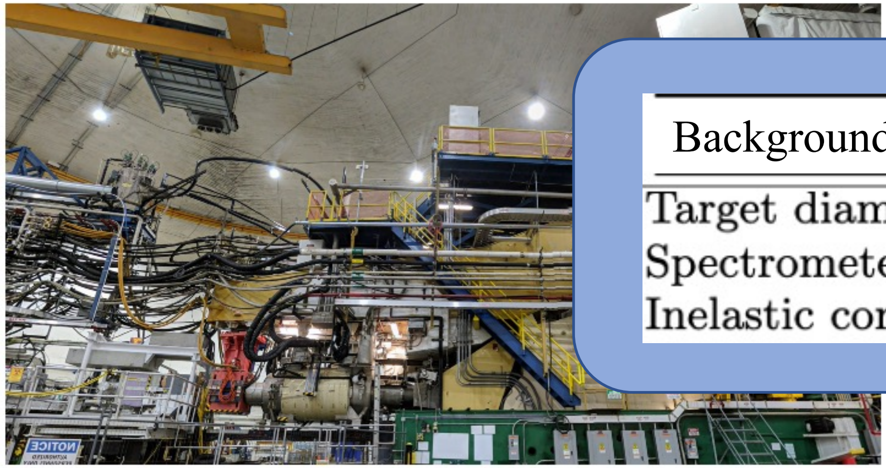

Background Correction	Absolute [ppb]	Relative [%]
Target diamond foils	0.7 ± 1.4	0.1 ± 0.3
Spectrometer rescattering	0.0 ± 0.1	0.0 ± 0.0
Inelastic contributions	0.0 ± 0.1	0.0 ± 0.0

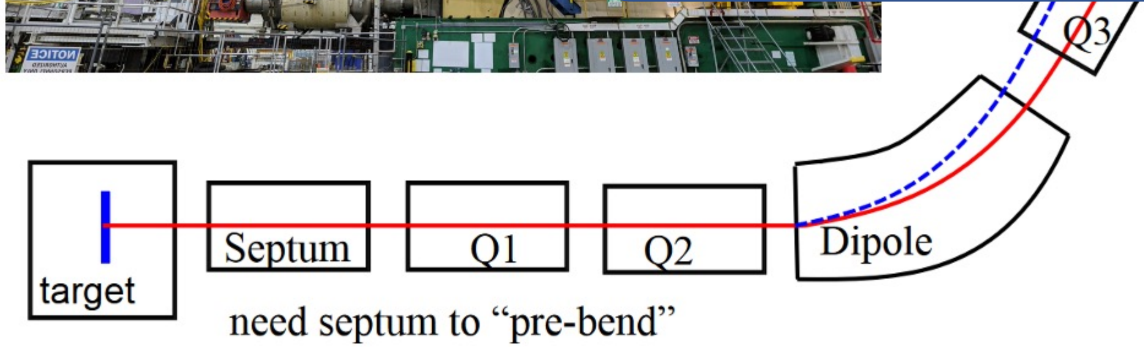

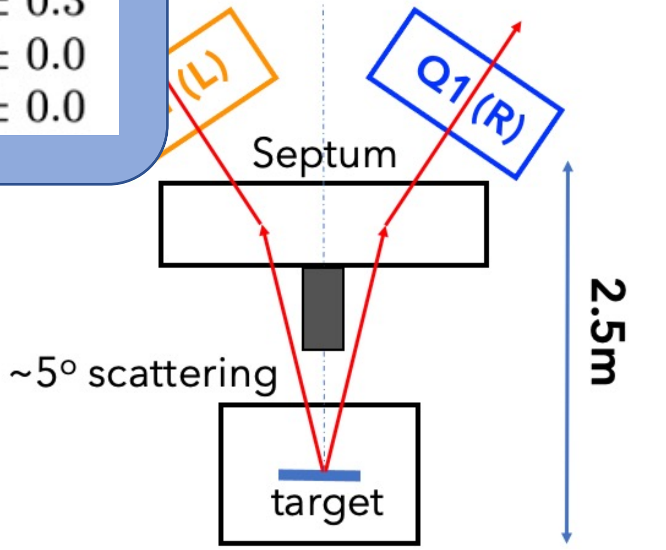

Almost there…

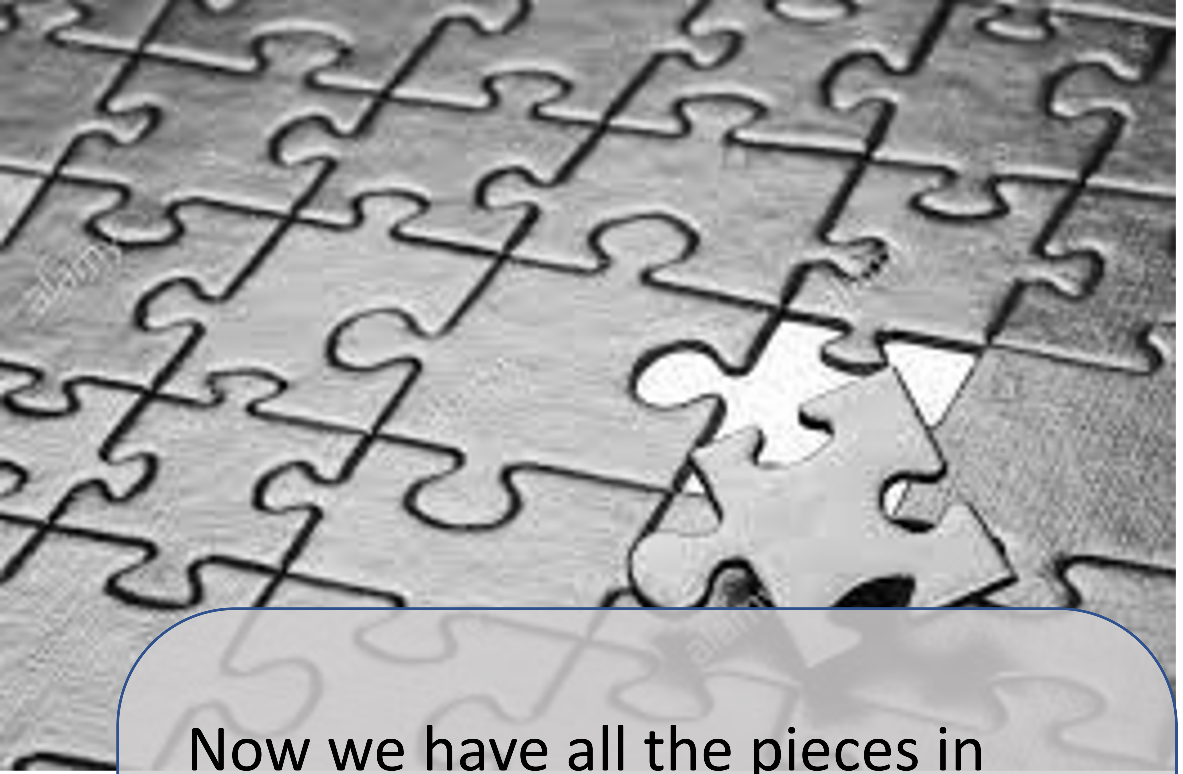

Now we have all the pieces in place to get A_{PV} from the raw measured asymmetry

$$A_{PV}^{\text{meas}} = \frac{1}{P_b}\frac{A_{\text{corr}} - P_b\sum_i A_i f_i}{1-\sum_i f_i}.$$

We still need Q^2 and an acceptance function to interpret this result in terms of neutron radius

$$A_{\text{PV}} = \frac{\sigma_R - \sigma_L}{\sigma_R + \sigma_L} \approx \frac{G_F Q^2 |Q_W|}{4\sqrt{2}\,\pi\alpha Z}\frac{F_{\text{W}}(Q^2)}{F_{\text{ch}}(Q^2)}$$

Determining central scattering angle and Q^2

Energy spectrum from water target

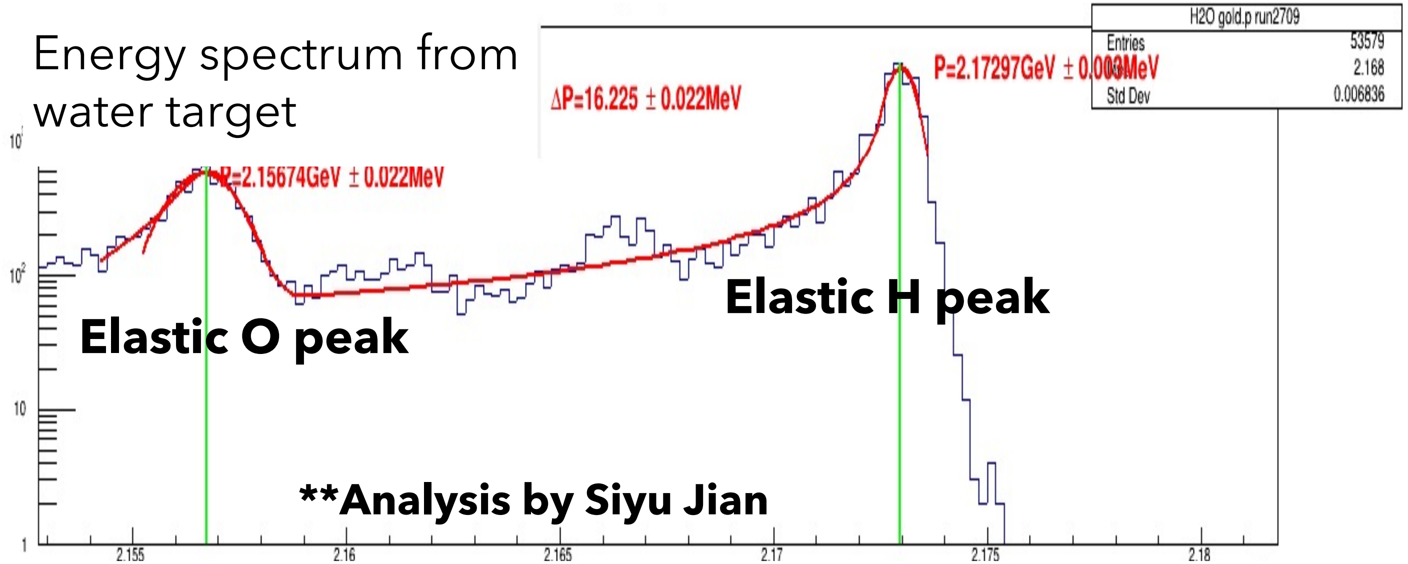

recoil momentum difference ⟶ scattering angle

$$\Delta E' = E'_O - E'_H = E\left(\frac{1}{1+\frac{2E\sin^2(\frac{\theta}{2})}{M_O}} - \frac{1}{1+\frac{2E\sin^2(\frac{\theta}{2})}{M_H}}\right)$$

- Critical to measure the absolute scattering angle to high precision
- Nuclear recoil method
- ^1H and ^{16}O in one target (same E-loss) provides straightforward measurement of angle, insensitive to other calibrations

$$A_{PV} \approx \frac{G_F Q^2}{4\pi\alpha\sqrt{2}} \frac{Q_W F_W(Q^2)}{Z F_{ch}(Q^2)}$$

- Determined central angle (4.76^0) to $\delta\theta = 0.02^0$
- $<Q^2> = 0.00616 \pm 0.00004$ GeV^2 ($\delta Q^2/Q^2 = 0.65\%$)

Concluding remarks

- PREX-2 successfully ran a technically difficult experiment thanks to the vigilance and consistent efforts of so many: students, post-docs, staff scientists, faculty, engineers, technicians, operators…
- One year after completing data taking was complete we unblinded the data (in spite of working through COVID-19 difficulties and strenuous efforts of largely the same crew simultaneously completing CREX)
- The final results were published in PRL in Feb 2021 and are already having an impact well beyond the Jefferson Lab and electron scattering community

Congratulations to our crew

Students: Devi Adhikari, Devaki Bhatta Pathak, Quinn Campagna, Yufan Chen, **Cameron Clarke**, Catherine Feldman, **Iris Halilovic**, **Siyu Jian**, **Eric King**, Carrington Metts, Marisa Petrusky, **Amali Premathilake**, **Victoria Owen**, **Robert Radloff**, **Sakib Rahman**, **Ryan Richards**, Ezekiel Wertz, **Tao Ye**, **Allison Zec**, **Weibin Zhang**




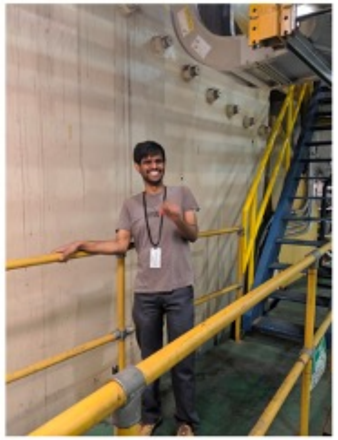


Post-docs and Run Coordinators: Rakitha Beminiwattha, Juan Carlos Cornejo, Mark-Macrae Dalton, Ciprian Gal, Chandan Ghosh, Donald Jones, Tyler Kutz, Hanjie Liu, Juliette Mammei, Dustin McNulty, Caryn Palatchi, Sanghwa Park, Ye Tian, Jinlong Zhang

Spokespeople: Kent Paschke (contact), Krishna Kumar, Robert Michaels, Paul A. Souder, Guido M. Urciuoli

Thanks to the Hall A techs, Machine Control, Yves Roblin, Jay Benesch and other Jefferson Lab staff

Special thanks to: Charles Horowitz and Jorge Piekarewicz for support and insightful conversations
Especially Chuck and grad student Brendan Reed who have worked to help us interpret our results

Backups

Correcting beam false asymmetries

Correct using measured sensitivities $\frac{\partial A}{\partial x_i}$:

$$A_{PV} = A_{meas} - \sum \frac{\partial A}{\partial x_i} \Delta x_i, \qquad x_i = x, y, x', y', E$$

Good agreement between three independent techniques for measuring sensitivities to beam parameters

1. Beam modulation
2. Linear regression
3. Lagrange Multiplier Regression

Left/right symmetry of detector provides some cancellation so correction dominated by energy

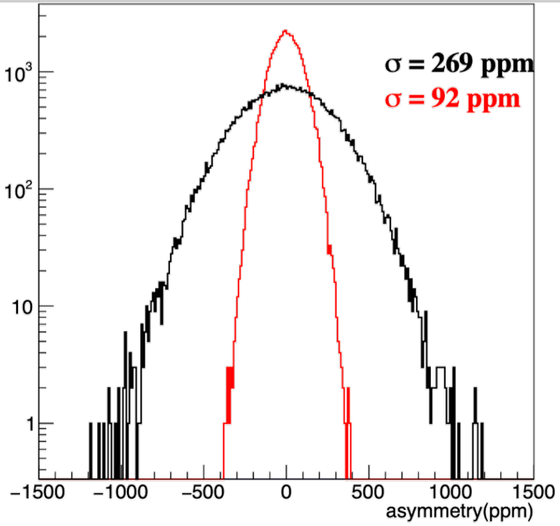

type	Mean(ppb)
X1	-22.33
Y1	22.5
E	-70.44
Y2	-2.84
X2	9.7
	1.27
	-0.01
Mostly BPM Electronic Noise	1.06
	0.26
	0.24
	0.18
	0.06
Total	-60.38

Total beam corrections: (60.4 ± 2.5) ppb

$A_{PV} = 550$ ppb

Other measurements sensitive to L

- Many other methods are more precise, but suffer from interpretability due to variable levels of model dependence
- PREX cleanly interpretable but less accuracy due to statistics

Donald Jones, SPIN 2021

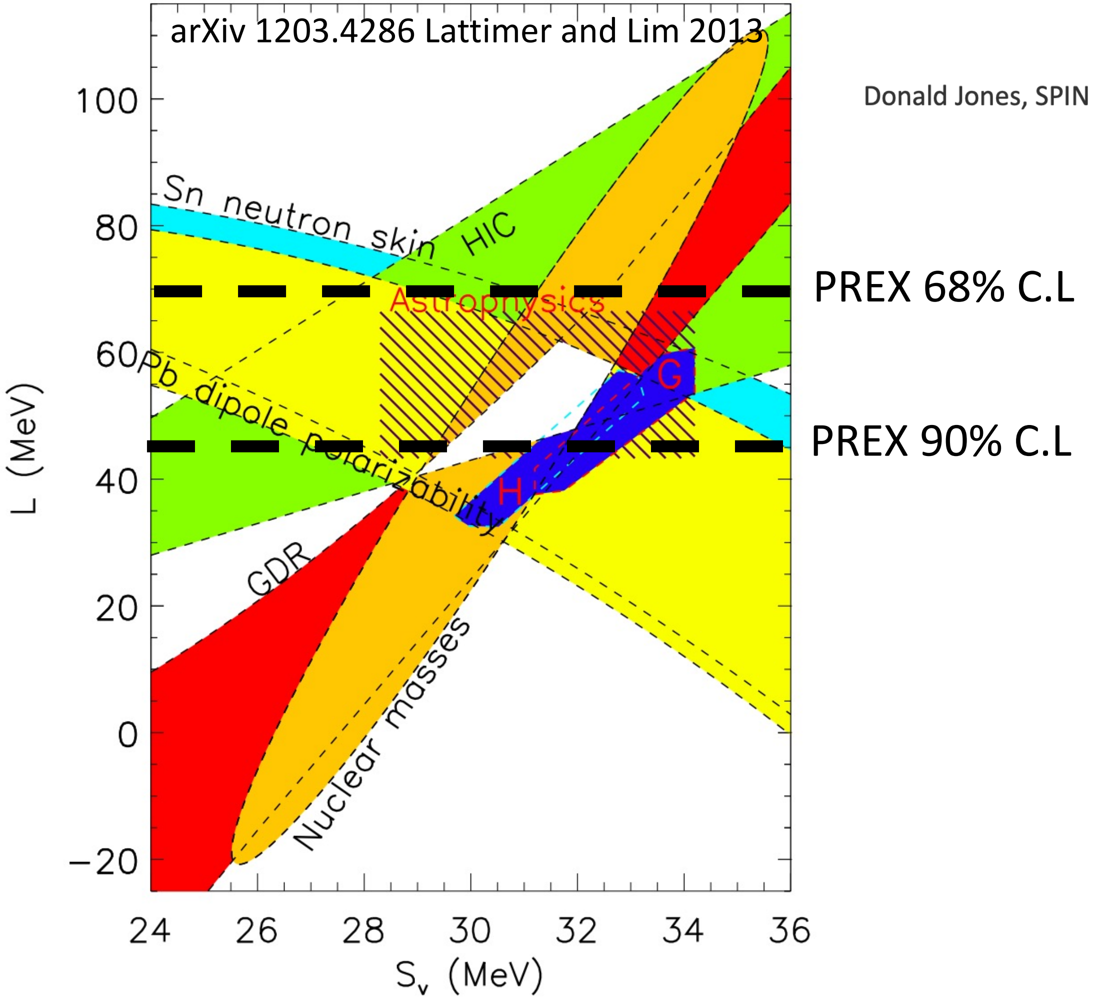

Fig. 2.— Summary of constraints on symmetry energy parameters. The filled ellipsoid indicate joint $S_v - L$ constraints from nuclear masses (Kortelainen et al. 2010). Filled bands show constraints from neutron skin thicknesses of Sn isotopes (Chen et al. 2010), the dipole polarizability of ^{208}Pb (Piekarewicz et al. 2012), giant dipole resonances (GDR) (Trippa, Coló and Vigezzi 2008), and isotope diffusion in heavy ion collisions (HIC) (Tsang et al. 2009). The hatched rectangle shows constraints from fitting astrophysical $M - R$ observations (Steiner, Lattimer and Brown 2010, 2013). The two closed regions show neutron matter constraints (H is Hebeler et al. (2010) and G is Gandolfi, Carlson and Reddy (2012)). The enclosed white area is the experimentally-allowed overlap region.